ELSEVIER

Increase of electrospray throughput using multiplexed microfabricated sources for the scalable generation of monodisperse droplets

Weiwei Deng[a], James F. Klemic[b], Xiaohui Li[b], Mark A. Reed[b], Alessandro Gomez[a],[*]

[a]Department of Mechanical Engineering, Yale University, New Haven, CT 06520-8286, USA
[b]Department of Electrical Engineering, Yale University, New Haven, CT 06520-8284, USA

Abstract

The development, fabrication, and testing of a compact multiplexed system of electrosprays are presented with the dual goal of increasing by orders of magnitude the liquid flow rate to be dispersed and of retaining the quasi-monodispersity of the generated droplets. The system was microfabricated as an array of nozzles etched in silicon, with a density of 250 sources/cm^2. Although the operation of a single electrospray is rather forgiving with respect to the electrode geometry, successful performance of the multiplexed system is critically dependent on a careful selection of the electrode configuration, which in the present work entails an extractor electrode mounted at a distance from the spray sources that is comparable to the distance between sources (on the order of 0.5 mm). The electrode has the dual function of limiting electric field cross-talk between neighboring sources and minimizing space charge feedback from the spray cloud. Measurements of current and droplet size as a function of flow rate and of droplet size distribution using ethanol demonstrated that the system may be optimized to produce uniform droplets simultaneously from all parallelized electrosprays, each one operating as an isolated spray in the quasi-monodisperse cone-jet mode. Ease of operation and uniformity in size from spray to spray require strategies to increase the pressure drop in the liquid flow path and/or to uniformize the electric field at the spray sources.
© 2005 Elsevier Ltd. All rights reserved.

Keywords: Electrospray; Multiplexing; Microfabrication; Monodisperse droplets; MEMS; Microfluidics

* Corresponding author. Tel.: +1 203 432 4384; fax: +1 203 432 7554.
E-mail address: Alessandro.Gomez@yale.edu (A. Gomez).

1. Introduction

A primary goal of fine particle synthesis is the ability to generate particles with narrow size distributions at flow rates adequate for various applications. This statement holds regardless of applications, from drug delivery, to the synthesis of nanoparticle ceramics, superconductors, quantum dots, photonic crystals and thin films. If one can tailor the size for a particular effect, for example, for the controlled/targeted drug release or to generate quantum dots with peculiar properties, the impact of fine particle synthesis will be dramatic. The present study focuses on the electrospray in the so-called cone-jet mode, a device that can produce monodisperse droplets/particles over a wide size range, from a few nanometers to hundreds of micrometers, depending on liquid flow rate, applied voltage and liquid electric conductivity. In particular, in the nanometric scale range, the capability of producing monodisperse particles with relative ease is unmatched by any other aerosol generation scheme. Our long-term goal is to remedy the main drawback that has hampered to date its widespread use in nanoparticle synthesis: low throughput.

Electrostatic means for liquid dispersion in minute droplets are used in a variety of technological applications (Bailey, 1988). In some systems, electric forces exclusively drive liquid dispersion, so that atomization and gas flow processes are relatively uncoupled. Such systems are referred to as electrosprays (ES). Within the electrospray class of atomizers is a particular type characterized by the additional feature of a tight control of the size distribution of the resulting aerosol. Such a system can be implemented by feeding a liquid with sufficient electric conductivity through a small opening, such as the tip of a capillary tube or a suitably treated "hole", maintained at several kilovolts relative to a ground electrode positioned at an appropriate distance from it. The liquid meniscus at the outlet of the capillary takes a conical shape under the action of the electric field, with a thin jet emerging from the cone tip. This jet breaks up further downstream into a spray of fine, charged droplets. Because of the morphology of the liquid meniscus, this regime is labeled as the *cone-jet* mode (Cloupeau & Prunet-Foch, 1989). Among the key features distinguishing the cone-jet electrospray from other atomization techniques are quasi-monodispersity of the droplets; Coulombic repulsion of the charged droplets, which induces spray self-dispersion, prevents droplet coalescence and enhances mixing with a secondary stream; and the use of a spray "nozzle" with a relatively large bore with respect to the size of the generated droplets, minimizing the liquid line obstruction risks.

Electrospray ionization mass spectrometry (ESI-MS), spearheaded by the pioneering work of Fenn at Yale in the 1980s (Fenn et al., 1989), is the *only* practical application of the electrospray in widespread use, as recognized by his 2002 Chemistry Nobel Prize. Key drawbacks that have hampered applications to other aerosol areas are, first and foremost, the low flow rates at which the cone-jet mode can be established and, to a lesser extent, the restrictions on the liquid physical properties of the liquids that can be dispersed with this technique. If such drawbacks are addressed and eliminated, the electrospray may find even greater use in a wide variety of applications, well beyond mass spectrometry.

Low flow rates represent a particularly severe drawback for applications requiring that the initial droplet size be small, as, for example, in drug inhalation or nanoparticle synthesis, which are areas of intense aerosol research. Since the electrospray exhibits a monotonic dependence of droplet size on flow rate (Chen et al., 1997; Tang & Gomez, 1995, 1996), if small droplets are needed to generate nanoparticles, mass flow rate may be minuscule (Gomez et al., 1997). The smaller the desired particle size, the smaller the mass flow rate. To provide quantities of nanoparticles suitable for biological tests, pharmaceutical treatment or other high-value-added applications, multiplexing the spray source is necessary.

The second drawback limits the applications to particle "precursors" that are well suited to dissolution in conducting fluids. If the goal is to generate very small droplets and ultimately nanoparticles, the conductivity of the working fluids may have to be relatively large, which may conflict with other constraints (e.g., pH-neutral solution in biomedical applications). Furthermore, in some applications organic and non-conductive buffers may be preferable, in which case the cone-jet electrospray would not be viable since its charging mechanism is inductive and requires a finite electric conductivity in the working fluid.

These two drawbacks have relegated the electrospray to the realm of academic curiosity, with the notable exception of mass spectrometry applications. Attempts to remedy the second shortcoming consist in having the working fluid with unsuitable properties "dragged" by an outer fluid with acceptable electrospray behavior in a two-fluid system (Loscertales et al., 2002; Smith, Barinaga, & Udseth, 1988). With respect to the flow rate limitations, the total flow rate to be dispersed in small droplets can be increased by multiplexing. This approach has been investigated with conventional machining to a limited degree (Almekinders & Jones, 1999; Kyritsis et al., 2002; Rulison & Flagan, 1993), in some cases without preserving monodispersity (Almekinders & Jones, 1999). It may also be impractical by more than one or two orders of magnitude, at least for typical configurations involving capillaries, nozzles or typical protrusions on which sprays are anchored. Further, the form factor of conventionally machined multiplexed systems limits practical scaling to relatively small amounts. A modestly multiplexed (by a factor of 9), but quite compact, system was developed by laser etching (Tang et al., 2001), with the goal of improving mass-spectrometry sensitivity in electrospray applications, rather than increasing the dispersed flow rates.

The task of dramatically increasing the throughput of electrospray systems, without sacrificing droplet monodispersity, may be addressed using microlithographic fabrication techniques developed for the field of MEMS (micro-electro mechanical systems) (Elwenspoek & Jansen, 1999; Madou, 1997). Namely, by adapting conventional silicon integrated circuit fabrication technology to the machining of mechanical structures in silicon and other materials, there is an opportunity of multiplexing electrospray devices at unparalleled scales, that is, by several orders of magnitude. Efforts using clean room technology in microfabricated electrospray systems have been previously pursued in mass spectrometry (Zhang et al., 2003), but also in that case the goal was to analyze a large batch of samples, one at a time, in an automatic way, rather than operating all of them in parallel. The dual goal of the present study is to increase by orders of magnitude the liquid flow rate to be dispersed and to retain the quasi-monodispersity of the generated droplets. Contrary to the operation of a single electrospray that is rather forgiving with respect to the electrode geometry, successful performance of the multiplexed system will be shown to be critically dependent on a careful selection of the electrode configuration. Measurements of spray current and droplet size distribution will be used to characterize the system aerosol performance.

2. Experimental approach

Multiplexed electrospray distributors were microfabricated in silicon using deep reactive ion etch (DRIE) of silicon wafers. Uniform nozzles, interspaced at various distances (2.52, 1.26 and 0.675 mm), and protruding from 150 to 450 μm were patterned with outer diameters ranging from 180 to 240 μm, and a fixed inner diameter of 120 μm. Fig. 1 sketches the specific microfabrication process flow used to fabricate the tested devices. Using double-sided wafer processing and deep reactive ion etching, a polished Si wafer with an oxide mask layer is patterned on both sides to realize nozzle arrays. DRIE of silicon can yield essentially straight sidewalls with large aspect ratios. Minimum feature sizes can be
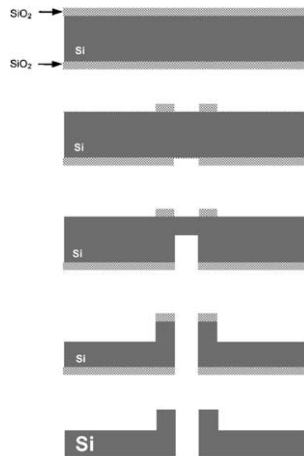
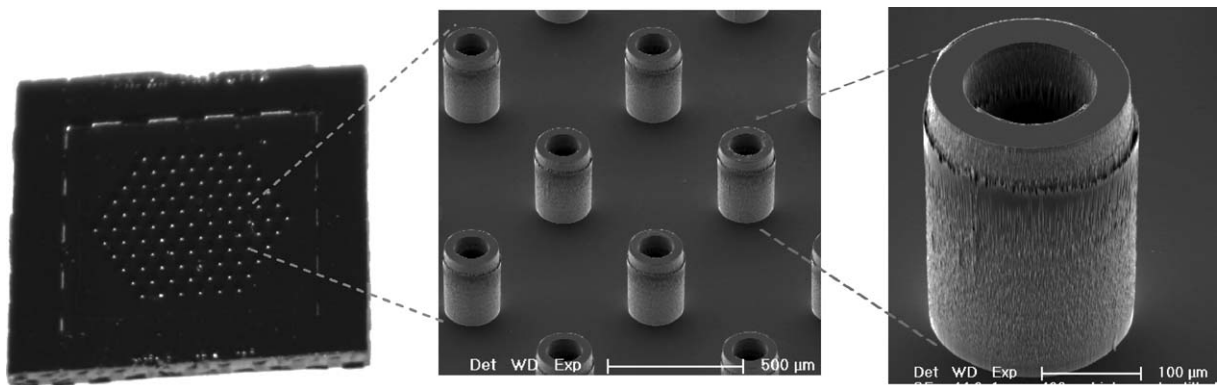Fig. 1. Microfabrication process flow used to fabricate the tested devices.

Fig. 2. Typical 91-nozzle system, with scanning electron micrographs of the nozzle array and of an individual nozzle.

on the order of $1\,\mu m$, which guarantees virtually identical protrusions, all acting as pseudo-capillaries. Fig. 2 shows scanning electron micrographs (SEMs) of a typical configuration, in this case a 91-nozzle hexagonally patterned arrangement. Excellent pattern transfer is evident on the individual nozzle SEM, with nearly vertical sidewalls in both the nozzle interior and exterior. The process allows for easy variation (e.g., nozzle scaling and array design) to optimize the intended application. Under certain conditions the reproducibility of geometric features between protrusions is an important prerequisite to equidistribution of flow rates among the multiplexed nozzles, and to the establishment of a controlled electric field at each nozzle, as will be discussed below.

A typical testing arrangement requires mounting the microfabricated distributor on a liquid reservoir, positioning suitable additional electrodes, and providing an electric connection to maintain the desired voltage drop between the distributor and the other electrodes. Details on the electrode configuration will be discussed in the following section. For all of the experiments discussed, we operated a multiplexed system of approximately $250\,\text{nozzles/cm}^2$, although higher and lower density multiplexed systems may be readily microfabricated in the same manner.

The current was measured by connecting the virtual ground to a voltmeter with known input impedance. Visual observation of the mode of operation was made possible by a laser beam focused by two lenses into a sheet parallel to the distributor surface and positioned a few millimeters downstream of the cone-jets. Scattering of the charged droplets in each spray resulted in the visualization of individual spray cross-sections appearing as small circular spots.

Tests were performed using ethanol, an alcohol with good electrospraying properties. The liquid was pumped continuously into the reservoir using a syringe pump with different syringe sizes to ensure that the plunger would be displaced at a reproducible and accurate speed. At the low flow rates, small (0.25 and 1 ml) syringes were used; the smaller the diameter of the syringe, the more accurate and steady the motion of the syringe plunger. As a result, the measurement of the current was more accurate and the range of stable flow rates for a given mode was increased. The liquid was sonicated for a few minutes prior to being loaded in the syringe slowly and steadily, to minimize the formation of microbubbles. Subsequently, the loaded syringe was sonicated for a few minutes to further eliminate possible microbubbles.

Droplet sizes were measured by a phase Doppler anemometer (Dantec, Electronik) capable of measuring simultaneously droplet size and two velocity components from the scattering of a frequency-modulated argon ion laser beam (Spectra Physics). The electrospray set-up was mounted on a multi-direction translational stage allowing for the systematic scanning of the spray by the laser probe volume. This volume was imaged on the receiver optics, which was coupled to photomultipliers for the signal recording and subsequent processing. A dedicated electronic processor sampled and analyzed the signal using Dantec BSA Flow Software. For each measurement, 5000 counts per sample were taken. Measurements were performed at a given flow rate by selecting the applied voltage so that the size distribution histogram would be as monodisperse as possible. In the cone-jet mode, although the bulk of the flow rate is dispersed in uniform size droplets, a small percentage may be dispersed as much smaller satellites that are electrostatically and inertially confined to the periphery of the spray (Tang & Gomez, 1994). To ensure that primary droplets were sized up, the laser probe volume was positioned along the axis of each spray.

3. Design criterion

A successful design should ensure that all nozzles operate simultaneously for a broad range of flow rates, with uniform droplet size from nozzle to nozzle, in a compact multiplexed system. In view of the monotonic dependence of droplet size on flow rate (Chen et al. 1997; Tang & Gomez, 1995, 1996), once the cone-jet regime is established, uniformity of droplet size for all nozzles imposes uniformity of flow rates. Fine tuning conditions in each nozzle, with independent control of flow rate and electric conditions, would pose prohibitive fabrication and operational challenges. An optimal design should ensure fabrication simplicity and nearly identical conditions for all nozzles.

A criterion can be formalized as follows. Consider the system illustrated in Fig. 3, highlighting a common feed tube, a reservoir with an optional flow homogenizer, the parallel nozzles and the cone-jet liquid/air interface. If we apply a momentum balance to the generic control volume CV_i, under steady state conditions and with negligible body forces, we obtain

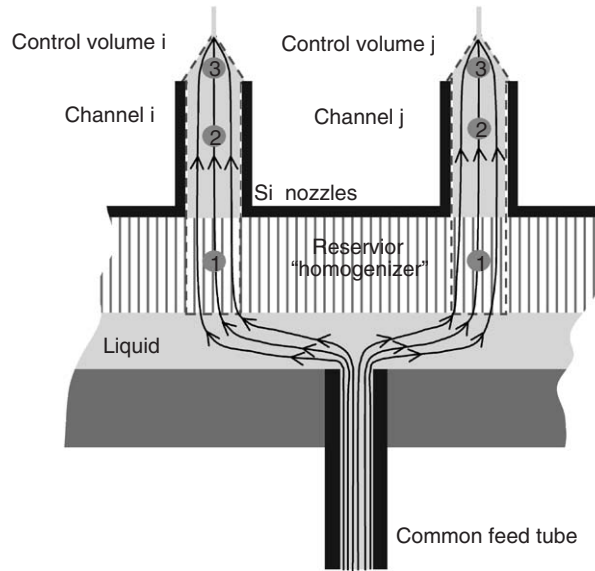$$\int_{CS_i} \vec{v} \rho \vec{v} \cdot d\vec{A} = \sum \vec{F}_{S_i},$$

Fig. 3. System schematic with fluid control volume.

where the term on the right-hand side combines all surface forces acting on the control surface CS_i bounding CV_i. If each parallel channel is to have the same flow rate, the inertia term on the left-hand side of the equation must be the same, regardless of the channel. The equidistribution of flow rates then implies that for the generic channels i and j

$$\sum \vec{F}_{S_i} = \sum \vec{F}_{S_j} = \sum \vec{F}_S = \vec{F}_{S_1} + \vec{F}_{S_2} + \vec{F}_{S_3},$$

where subscript i and j can be dropped, and the last equality refers to the decomposition of the total surface forces in each channel into three contributions: $\vec{F}_{S_1}$, $\vec{F}_{S_2}$ and $\vec{F}_{S_3}$, referring to the homogenizer region, the nozzle and the cone-jet interface, respectively. In region 1, only pressure and viscous forces are at play with the establishment of a pressure drop to overcome viscous losses. In region 2, similar considerations apply, with the establishment of the well-known Hagen–Poiseille flow at the prevailing Reynolds numbers of unity order. In region 3, capillary forces and electrohydrodynamic normal and shear stresses at the liquid/air interface are important and would need to be integrated on the liquid/air interface. Capillary forces depend on the liquid surface tension and on the interface geometry. Electro-hydrodynamic stresses depend on the electric field at the nozzle outlet. Implicit in this argument is that the electric charge has relaxed to the fluid/air interface, as typical of the stable cone-jet electrospray regime.

In region 1, uniformity of the pressure drop across the homogenizer would be required with the insertion of baffles, honeycombs, beads, frits and other obstructions that would ensure that there are no preferential paths from the feed tube outlet to each nozzle. However, if $\vec{F}_{S_2} \gg \vec{F}_{S_3}$, there would not even be need for a homogenizer since the prevailing Reynolds number in the fluid reservoir is of order 10^{-2} and one would expect a uniform Stokes regime, with no separation at the walls and $\vec{F}_{S_1} \approx 0$. The condition $\vec{F}_{S_2} \gg \vec{F}_{S_3}$ can be reached by judicious selection of the inner diameter of the parallel nozzles and flow uniformity from nozzle to nozzle would be guaranteed by the high spatial resolution of microfabrication. With either

$\vec{F}_{S_1}$ or $\vec{F}_{S_2}$ or both much larger than $\vec{F}_{S_3}$, the system should be relatively uninfluenced by edge effects in the electric field distribution affecting $\vec{F}_{S_3}$ (see Fig. 5) and the requirement on the electric field is that it be sufficiently intense for the cone-jet to be established at each nozzle.

If neither of the conditions above is fulfilled, the following situation ensues. For a given interface geometry and liquid surface tension, capillary forces are fixed. Particularly important now become the electrohydrodynamic stresses that extrude the fluid into a ligament that is orders of magnitude smaller than the nozzle bore. In such a case, great care must be taken to ensure that the electric field does not vary significantly from nozzle to nozzle, since this field controls not only the establishment of the cone-jet regime, but also the liquid flow rate that is drawn from each nozzle.

To establish an intense electric field, the simplest configuration would entail mounting a flat electrode at a distance from the multiplexed distributor. The distance selection is critical, since a few characteristic length scales are already apparent in the distributor design: the inter-nozzle distance, l_{in}, the nozzle protrusion, h, and the nozzle diameter, D. Microfabrication allows for the manufacturing of essentially planar structures, with protrusions limited by the wafer thickness. In the present system, h was limited to 0.45 mm, which for the densest packing is of the same order as the inter-nozzle distance, l_{in}, at 0.675 mm. If the flat electrode is mounted at a distance $L \gg h$, the effect of the protrusion would be irrelevant and the electric field established would essentially be that which is between two capacitor plates. It is doubtful that with such a configuration sufficiently intense electric fields can be established for the cone-jet mode of operation, before the onset of corona breakdown in the surrounding gas. Furthermore, feedback from space charge may become inevitable.

If, on the other hand, $L \sim h \ll l_{in}$, the effect of the protrusions will be significant and the field can be localized with minimal influence of the neighboring nozzles. Inevitable flooding of the liquid flowing through the system would prevent operation with a ground electrode a fraction of a millimeter away from the nozzle. If a ring electrode to let the fluid through a small opening is used, the cone-jet can be established and a spray with the appropriate properties for a given application can be formed. This configuration, often called "extractor electrode", is typically used in electron beam applications. It was also used in early electrospray applications to electric propulsion (e.g., Hendricks, 1962) and combustion (e.g., Chen & Gomez, 1996). The generated droplets would eventually reverse their paths and be attracted back to the lower potential electrode, causing flooding and eventual interruption of the flow. This effect can be avoided if an additional electrode is put in place at an even lower potential to "sweep" the droplets away and use them for the intended applications. This can be combined also with an external flow that would drag the droplet away overcoming electrostatic attractive forces. The additional advantage of this configuration is that it shields the cone-jet region at the source of the spray from the region where the spray cloud disperses, with attending space charge. A separation of the cone-jet region from the spray utilization region is generally desirable for stability and application considerations.

The chosen electrode configuration is depicted in the schematic in Fig. 4(a). The microfabricated Si distributor is charged at about 1 kV potential above that of a metal ring extractor plate positioned at a distance of typically 200–500 μm by means of a glass insulator spacer, under conditions in which $L < h < l_{in}$. Since L is only a factor of 3 smaller than l_{in}, it is likely that nozzle cross-talk may not be completely eliminated. The stainless steel ring extractor itself was designed and microfabricated using photolithography and metal etching to tolerances compatible with the microfabricated nozzle array. Visible in the schematic is a ground electrode several millimeters downstream. Comments on the other two configurations in Fig. 4 will be made in the discussion of Fig. 5 below.
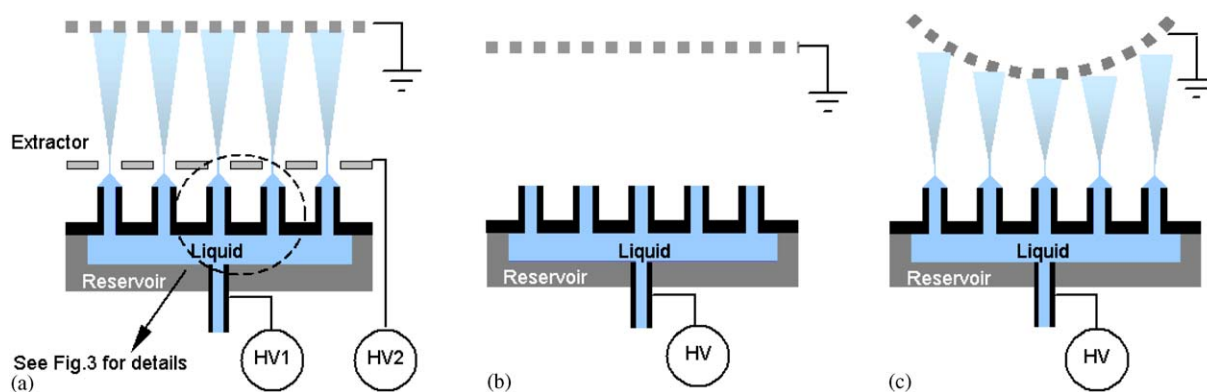
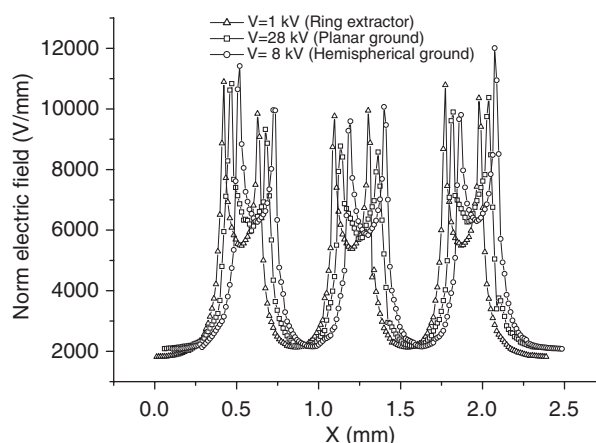Fig. 4. Schematic of various electrode configurations.

Fig. 5. Comparison of the electric field at the outer nozzle and at the central one in a system of seven nozzles for the three electrode geometries in Fig. 4.

4. Results and discussion

4.1. Electrostatics modeling of various configurations

Modeling of the external electric field using FEMLAB (COMSOL Inc., 2005) provided supporting evidence of the electric field design criterion. We underline the qualitative nature of these calculations, since the presence of the liquid and its coupling with the electric field are unaccounted for and poses a much more challenging problem. Even if the governing equations and boundary conditions were properly specified in the full electrohydrodynamic problem, the disparity of length scales would dictate a very challenging computational approach, since these devices span four orders of magnitude from the micrometer size liquid-drop ligament at the breakup point (the critical region where electrospray forms) to the several millimeters of the overall device domain size. The difficulties would be compounded further

by the need to capture the transient behavior of the system, with the instabilities that limit its behavior, and the presence of moving boundaries at the fluid/gas interface.

Simple electrostatic modeling is revealing in explaining some of the experimental observations. To that end, solutions of the Laplace equation $\Delta\phi = 0$ for the electric potential ϕ were computed using FEMLAB for a simplified geometry consisting of seven nozzles protruding from a distributor plate. The electric field was computed by post-processing the potential field. Computations were performed for three cases: the extractor electrode that was described in detail in the preceding discussion (Fig. 4a); simple flat electrode at a working distance of 1 cm from the wafer, as a reference case (Fig. 4b); and a ground electrode shaped as a paraboloid to decrease the distance between the innermost nozzles and the ground, as compared to that of the outermost nozzles (Fig. 4c), for reasons to be discussed below. The voltage levels in the three cases were chosen so that the electric fields at the nozzles would be comparable in the three cases. In the second case the wafer was charged at 28 kV with respect to a flat ground electrode 1 cm away; in the third one, it was charged at 8 kV with respect to a hemispherical ground electrode, the bottom of which was 3 mm away from the wafer. Fig. 5 shows the electric field at the three nozzles where the cone-jet would be formed.

Notice that to achieve approximately the same field, one needs extremely high voltages in the second case (Fig. 4). In a typical startup procedure in such a configuration, the outer nozzles in the array would electrospray first, as a consequence of the more intense field locally (see below), whereas the innermost nozzles would fail to operate leading to flooding of the distributor with the formation of a liquid layer that could not be disrupted into controlled and properly anchored electrosprays. Increasing the voltage to the extremely high values used in the calculations would not be practical. Sharp corners in contact with the charged electrode, contact wires, or even surface irregularities resulting from microfabrication can cause corona discharge in the surrounding gas. This configuration failed to work in preliminary attempts. In the third case (Fig. 4c), in which the ground electrode was properly shaped to enhance the homogeneity in electric field among the nozzles and reduce the applied potential to approximately 8 kV, we managed to get all sprays to "fire" at the same time. With the ring extractor and the paraboloid ground configurations the degree of nonuniformity in the field between the side nozzles and the central one is reduced from 22% in the case of the flat electrode (Fig. 4b) to approximately 10%, which may explain why these configurations were successful. However, the paraboloid geometry proved impractical since operation could be established for brief periods of time before electrode flooding would ensue. Furthermore, the geometry of the ground electrode may have to be tailored to a particular liquid flow rate and liquid conductivity, since both variables may affect the space charge field.

The electric field comparison in Fig. 5 suggested that the ring extractor configuration, is the most promising; consequently, it was used in all subsequent tests. Fig. 6 shows pictures of the microfabricated distributor, with the customary penny as size standard, and of the system in operation with a multitude of sprays issuing from the system.

4.2. $\vec{F}_{S_1} \approx 0$, $\vec{F}_{S_2}$ comparable to $\vec{F}_{S_3}$: critical role of the external electric field

Let us consider the limiting case, $\vec{F}_{S_1} \approx 0$, in which there is no homogenizer and the pressure drop in the nozzles does not overwhelm interfacial forces. As discussed earlier, electrohydrodynamic stresses that depend on the electric field at the nozzle are particularly important in this case since this field controls not only the establishment of the cone-jet regime, but also the liquid flow rate that is drawn from each nozzle. The electric field is due to the electric potential applied between electrodes, the so-called external
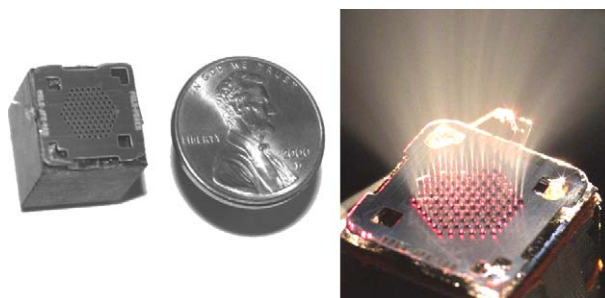
Fig. 6. (a) Microfabricated distributor, with the penny as size standard, and (b) system in operation with a multitude of sprays.
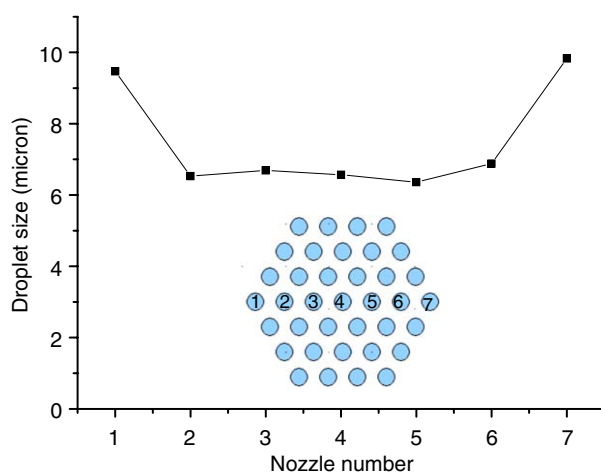

Fig. 7. Average droplet diameter in individual cone-jet electrosprays in the multiplexed mode.

field, and can be mitigated by the space charge field that is due to the charged droplet cloud downstream, if the extractor electrode is inadequate to shield the cone-jet from the cloud (Tang & Gomez, 1994). In the present experiments characterized by liquids of relatively modest conductivity, space charge does not appear to be an issue. Its feedback may become non-negligible as the current through the system increases and at some point it may even hinder the system operation.

As long as the external electric field is the same at each nozzle, the goal of uniform flow rates and droplet size can be achieved. However, the calculations discussed in Fig. 5 already show that edge effects may be inevitable, with the electrostatic pull in the outermost array of nozzles being stronger, which should result in larger flow rates and droplet size. We will now see indirect experimental confirmation of this nonuniformity. To ease the monitoring of the system, we cut the outermost nozzles to leave an hexagonal pattern of 37 nozzles. Fig. 7 shows the droplet average diameter measured in a scan across the hexagon with nozzle numbers identified in the inset in the figure. As anticipated, the outermost nozzles pass a higher flow rate and generate larger droplets, which is entirely consistent with the external field electrostatic pattern in Fig. 5.

Further evidence of the importance of the external field uniformity is provided by the "firing" pattern of the multiplexed system as the flow rate is increased. Fig. 8 shows the scattering pattern observed as
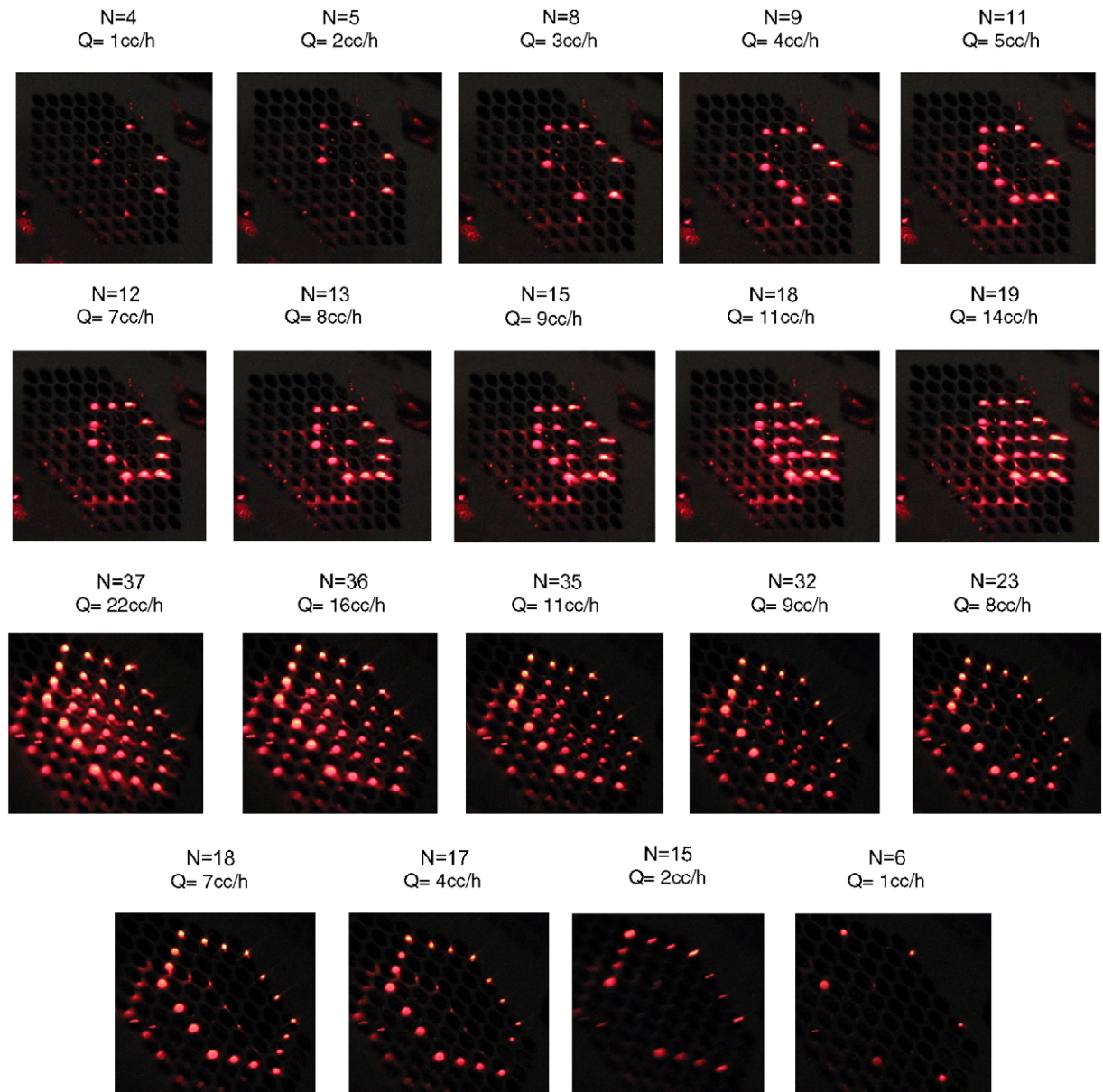
Fig. 8. "Firing" pattern of the extractor electrode system as the flow rate is either increased (top two rows) or decreased (bottom two rows). Red dots are due to the scattering from each spray droplets off a He–Ne laser sheet parallel to the distributor. Note: dot pattern is duplicated via reflection from the shiny metal extractor electrode surface, as faintly visible on the left of each image.

a laser sheet is shone parallel to the distributor surface. The top two rows of figures show the pattern obtained as the flow rate is increased at a fixed voltage difference between distributor and the extractor ring. The bottom two rows pertain to the pattern obtained as the flow rate is decreased. Also, in this case experiments were conducted with arrays of either two or three hexagonally configured and concentric
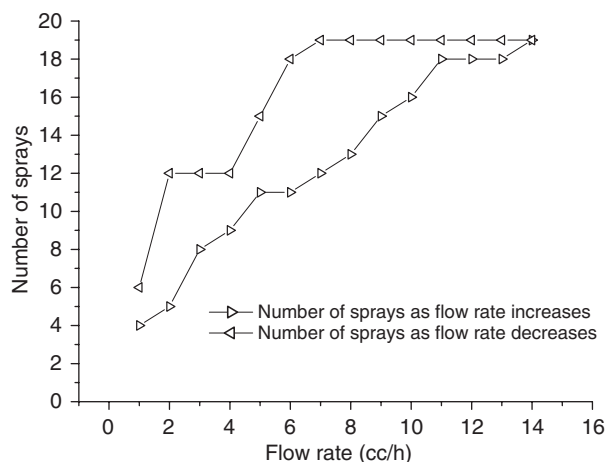
Fig. 9. Hysteresis in the "firing" pattern as the liquid flow rate is first increased and then decreased.

nozzles, obtained from the initial distributor by selectively cutting the outermost nozzles. Note that the pattern in each figure is mirrored by the reflection on the shiny metal extractor electrode surface on the left of each image. It is observed that, as a function of flow rate, the outermost nozzles at the vertices of the hexagon begin to fire first (top left). As the flow rate is increased, the other nozzles in the outermost "ring" gradually turned on. Next, the central nozzle begins to fire and finally the intermediate "ring" is turned on, until all 19 nozzles are "firing" at the same time. Most interesting is the hysteretic pattern with respect to the number of jets that are simultaneously operating, which is a function of whether a particular flow rate is achieved by decreasing or increasing the liquid pumped through the system. As shown in Fig. 9 for the system of 19 electrosprays, there is a monotonic dependence of number of jets operating on flow rate as the flow rate is increased. Once all jets have been turned on, the flow rate can be decreased by more than a factor of two before any electrospray disappears. In other words, the average flow rate needed to generate a new spray at a nozzle is higher than the average flow rate to keep a spray. Furthermore, when a mechanical and/or electrical perturbation is introduced (e.g., by tapping the fluid reservoir, or introducing a metal tip in the vicinity of non-operating nozzles), more cone-jets can be turned on (as compared to the data in Fig. 9).

Fig. 10 shows details of the electric field computed on each of the nozzles in the 19-nozzle hexagonal pattern, with numbering of different profiles in correspondence of different nozzle types (e.g., at a vertex of the hexagon, at the center, etc.). Somewhat surprisingly, the "firing" pattern in Fig. 8 (top row) for increasing flow rate is entirely consistent with the hierarchy of intensity of electric field at the nozzle outlets. This observation suggests that, first, space charge is not controlling the system performance, as intended by the selection of the extractor electrode design. Second, it shows that details of the cone-jet morphology and of the potential drop through the quasi-equipotential liquid are not critical. If this is the case, further fine-tuning of the microfabrication design, which may be planned in the future by simply using FEMLAB and solving Laplace equation for different geometries, can yield greater uniformity in both firing pattern and droplet size.

We also notice that the greatest nonuniformity in the field is between the outermost "ring" and the rest of the nozzles. If such nozzles are plugged, greater droplet uniformity would ensue at the cost of sacrificing some of the microfabricated nozzles. Fig. 11 demonstrates this feature for a system of 61
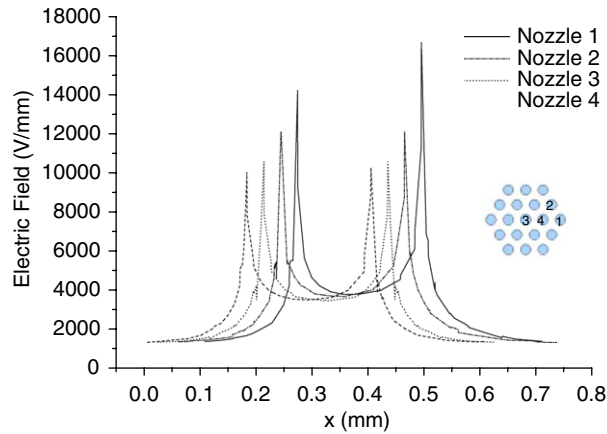
Fig. 10. Details of the electric field computed on each of the nozzles in a 19-nozzle hexagonal pattern. Numbering corresponds to different positions of the nozzles, as shown in the inset.
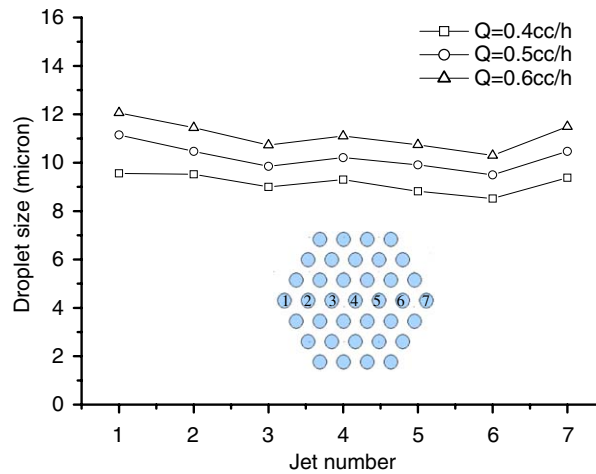

Fig. 11. Average droplet diameter in individual cone-jet electrosprays in the multiplexed mode with the outer "ring" of plugged "dummy" nozzles.

nozzles, the outer ring of which consisted of 24 plugged nozzles, leaving the remaining 37 in operation. To quantify the size scatter from jet to jet, a relative standard deviation (RSD) for the average droplet size of all operating sprays is defined as

$$\text{RSD} = \frac{1}{\bar{D}} \sqrt{\left. \sum_{i=1}^{N} (\bar{D}_i - \bar{D})^2 \right/ (n-1)},$$

where $\bar{D}_i$ is the average droplet diameter for jet i, and $\bar{D} = \sum \bar{D}_i / n$ is the droplet size averaged over all jets. The uniformity of the droplet size is good, with the RSD < 0.053, which is comparable to the

Table 1
Average droplet size and relative standard deviation (RSD) for the conditions of Fig. 11

Nozzle number	$\bar{d}(\mu m)$	RSD
$\dot{Q} = 0.4\,cc/h,\ \bar{D} = 9.16\,\mu m$		
1	9.56	0.07
2	9.52	0.08
3	9	0.08
4	9.3	0.09
5	8.82	0.09
6	8.52	0.10
7	9.38	0.09
$\dot{Q} = 0.5\,cc/h,\ \bar{D} = 10.22\,\mu m$		
1	11.15	0.08
2	10.47	0.08
3	9.85	0.09
4	10.21	0.10
5	9.91	0.10
6	9.5	0.08
7	10.47	0.09
$\dot{Q} = 0.6\,cc/h,\ \bar{D} = 11.12\,\mu m$		
1	12.06	0.08
2	11.45	0.09
3	10.73	0.09
4	11.1	0.10
5	10.74	0.11
6	10.3	0.09
7	11.49	0.09

degree of non-uniformity in size within a single jet, as measured by an RSD of 0.09, attesting to the quasi-monodispersity requirement. Table 1 provides further details. Notice that even the small changes in droplet size from nozzle to nozzle seem to be consistent with the hierarchy of electric field intensity in Fig. 10, with a relative maximum in correspondence of the central nozzle.

4.3. Current measurements

To characterize the multiplexed system quantitatively, under the same conditions as in the preceding section and with the outermost nozzles plugged, we related the behavior of the multi-jet regime to the better-known single electrospray cone-jet mode. To that end, the average current per jet was compared to that measured in a separate experiment in which all protrusions but one were cut off and the corresponding holes plugged, to generate a single cone-jet regime. With the electrospray in the multiplexed regime, the total current was measured and the number of jets was counted, with the ratio of the values yielding the average current per jet. Results are plotted in Fig. 12. Although considerable work has been made in deriving scaling laws for different liquids that are largely based on dimensional analysis, in the present case we will refrain from applying such laws since no comparisons with other fluids will be made. Thus it suffices to compare the relative behavior of the multiplexed mode versus the single cone-jet counterpart.
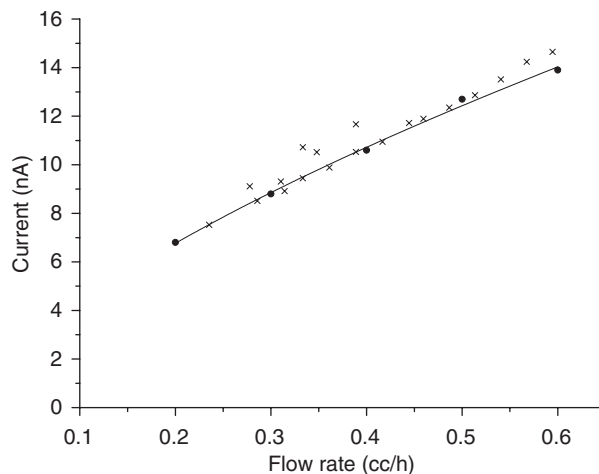
Fig. 12. Average current per jet versus average flow rate per jet for multiplexed ($\times$) and single ($\bullet$) cone-jet ethanol electrosprays.

It appears that the average current per jet obeys the same power law as in the single cone-jet mode, which suggests that space charge is not limiting under the present conditions and that each cone-jet behaves in the same way, regardless of the mode. The power law dependence of Fig. 12 can be further analyzed, as follows:

$$I = \sum_{1}^{n} I_i \propto \sum_{1}^{n} \dot{Q}_i^{\alpha} = \sum_{1}^{n} \left(\frac{\dot{Q}}{n}\right)^{\alpha} = n^{(1-\alpha)} \dot{Q}^{\alpha},$$

where α is the exponent of the power law in Fig. 11, n is the number of jets, $\dot{Q}$ is the total liquid flow rate, and $\dot{Q}_i$ is the flow rate through the i cone-jet. The second equality is implicitly assuming that the flow rate is uniformly distributed among the n cone-jets, as shown above. The implication of the above equation is that if the application requires the highest possible charging of the liquid, as for example in ESI-MS, the multiplexed mode will yield a current gain by a factor $n^{1-\alpha}$ in the current passed through the spray, where α is invariably less than unity and in the present case close to 0.5. Consequently, at a constant flow rate, we anticipate that the current monotonically increases with the number of jets and the multiplexing level.

4.4. $\vec{F}_{S_1} \gg \vec{F}_{S_2}, \vec{F}_{S_3}$: performance with flow homogenizer

As discussed earlier, to achieve a more uniform behavior and minimize the criticality in the uniformity of the electric field from nozzle to nozzle, one can revisit the momentum balance and consider the other limiting case, either with a homogenizer in the reservoir that introduces a pressure drop such that $\vec{F}_{S_1} \gg \vec{F}_{S_2}, \vec{F}_{S_3}$ or using nozzles that have sufficiently small inner diameter so that $\vec{F}_{S_2} \gg \vec{F}_{S_3}$. In both cases, the system performance would be freed from the influence of edge effects in the electric field distribution and the "firing" pattern should improve. The second option would require changes in microfabrication that were not contemplated in the present study although they may be included in future designs. The first option, on the other hand, was readily implemented by inserting glass beads measuring 0.25 mm in

average diameter and sandwiching them between stainless steel filter grade woven wire cloths with 26 μm opening width. With this modification, all 91 nozzles fired simultaneously at a minimum average flow rate of 0.275 cc/h, which is comparable to the minimum flow rate of an isolated cone-jet electrospray (0.2 cc/h). The spread in average size from jet to jet was found to be more pronounced than under the conditions of Fig. 10, with an RSD of 0.21, even though each jet was still quasi-monodisperse with a typical RSD < 0.15. The reason for the greater nonuniformity is that the nozzle inner diameter, the glass beads and the mesh holes are all comparable in size. As a result, the packed bed fails to deliver the liquid evenly, i.e., at the same flow rate for each nozzle, but nevertheless downplays the role of electric field nonuniformities in nozzle "misfire". This undesirable behavior should be easily remedied by improving the design of a relatively high-pressure drop flow homogenizer, for example, by using ultrafine porous filters.

4.5. Multiplexing scale-up and potential applications

We should now compare the present effort in multiplexing with a concurrent study (Bocanegra, Galán, Márquez, Loscertales, & Barrero, 2005), in which nozzles, capillaries or any kind of protrusions were dispensed with and the multiplexed cone-jets were anchored on holes drilled in materials that were not wetted by the liquid to be dispersed (Lozano et al., 2004). Using CNC fabrication they reported a respectable multiplexing density of 115 emitters/cm^2, a factor of 2 smaller than in the present study. The trade-off is between less expensive manufacturing in their system, with some limitations in the type of liquid to be dispersed, based on its wetting characteristics, and the denser microfabrication pursued here that can be used with any electrosprayable fluid, but is certainly more elaborate and expensive, at least at the prototype stage. On this point, we can add two additional considerations that make the microfabricated route more appealing: first, microfabrication is a batch processing method and offers unique economies of scale as a manufacturing method; second, it is also possible to simplify the fabrication even at this prototype stage, by using a micromachined silicon master as a mold for the construction of distributors in other materials. Micromolding from microfabricated silicon masters has been used for high fidelity fabrication in elastomers (Xia & Whitesides, 1998; Klemic et al., 2002) as well as other polymers (Xia & Whitesides, 1998) and ceramics (Liew et al., 2001). In this context, it is not necessary that the distributor be made of a conducting material. Experiments dating back to the pioneering work of Zeleny (1915) show that one can operate the system by burying the high-voltage electrode within the liquid and using insulating surfaces for the liquid distributor.

Using microlithographic fabrication, one may multiplex by several orders of magnitudes by using the same nozzle density and identical fabrication process. For example, maintaining the same packing density, but applying the mask to an entire wafer, with a diameter of approximately 10 cm, would yield the realization of 2.0×10^4 parallel sources in a relatively small footprint. This consideration may shed light on applications that can benefit from this development. It is unlikely that large-scale applications such as fuel dispersion in gas turbines will ever be candidates, since individual nozzles can issue on the order of 1 cc/h of fuel or less for small droplet generation. Small-scale combustion applications for liquid-fueled batteries, which originally motivated this study, are a much better prospective (Kyritsis et al., 2004). More generally, it is likely that the electrospray will remain still somewhat limited in flow rate. Therefore, the largest payoff may stem from applications in the high-tech/high value-added category, such as nanoparticle synthesis, in which the electrospray capability of tight control in size distribution has already been demonstrated (Chen et al., 1995; Loscertales & Fernández de la Mora,

1993). Examples include nanoparticle synthesis of biomaterials (Gomez et al., 1997), high-temperature synthesis by electrospray pyrolysis of ceramic oxides (Mädler et al., 2002a), quantum dots (Lenggoro et al., 2000) and metal oxides (Mädler et al., 2002b), electrospray coating techniques (Kaelin et al., 2004) and nanofiber synthesis by electrospinning (Zhang et al., 2005).

5. Conclusions

The development of a parallelized electrospray dispersion system was demonstrated, with the dual goal of increasing by orders of magnitude the liquid flow rate to be dispersed and of retaining the quasi-monodispersity of the generated droplets. Although the operation of a single electrospray is rather forgiving with respect to the electrode geometry, successful performance of the multiplexed system is critically dependent on a careful selection of the electrode configuration. The latter consisted of identical nozzles multiplexed into a parallel array that was batch-microfabricated in silicon by deep reactive ion etching and an extractor electrode plate with multiple holes, each positioned concentrically with each upstream nozzle. The plate was positioned at a distance on the same order as the inter-nozzle distance (approximately 0.5 mm), with the dual function of limiting cross-talk between neighboring sprays and minimizing space charge feedback by shielding the region where the electrospray cone-jet is formed from that where the majority of the spray cloud is present. A remarkable packing density of 250 nozzles/cm^2 was achieved, which permits multiplexing by several orders of magnitude in a relatively small footprint. Under optimal conditions, an individual electrospray is anchored on each nozzle. Testing with ethanol demonstrated that the system produces uniform average droplet size from spray to spray. The current dependence on the average flow rate per nozzle is the same as that of a single (non-multiplexed) electrospray, providing supporting evidence that all electrosprays are in the cone-jet mode. Measurements of the size distribution in radial scans parallel to the surface of the liquid distributor showed an RSD of 0.05, based on the spread of the average droplet size from each electrospray, with each electrospray having a typical RSD of 0.1, confirming the generation of virtually monodisperse droplets. Good performance of the system requires minimization of edge effects and potential nonuniformities in the feed stream flow rate distribution. The observed dependence of active, i.e., electrospraying, nozzles on flow rate, under conditions in which no efforts were made to increase the pressure drop in the liquid reservoir, correlates with non-uniformities in the external electric field from nozzle to nozzle. This result suggests that further tailoring of the microfabrication effort by routine computation of solutions of Laplace equation for the electric potential may be surprisingly helpful in altogether eliminating electric field edge effects. Alternatively, the system dependence on nonuniformities in the electric field may be suppressed by deliberately introducing homogenous flow resistance either in the fluid reservoir or across the nozzles.

References

Almekinders, J. C., & Jones, C. (1999). Multiple jet electrohydrodynamic spraying and applications. *Journal of Aerosol Science*, *30*, 969–971.

Bailey, A. G. (1988). *Electrostatic spraying of liquids*. UK: Research Studies Press Ltd.

Bocanegra, R., Galán, D., Márquez, M., Loscertales, I.G., & Barrero, A. (2005). Multiple electrosprays emitted from an array of holes. *Journal of Aerosol Science*, in press.

Chen, G., & Gomez, A. (1996). Co-flow laminar diffusion flames of monodisperse sprays: Structure, evaporation and microgravity effects. *Combustion Science and Technology*, *115*, 177.

Chen, D. et al. (1995). Electrospraying of conducting liquids for monodisperse aerosol generation in the 4 nm to 1.8 mm diameter range. *Journal of Aerosol Science*, *26*, 963–977.

Chen, D. et al. (1997). Experimental investigation of scaling laws for electrospraying: Dielectric constant effect. *Aerosol Science and Technology*, *27*, 367–380.

Cloupeau, M., & Prunet-Foch, B. (1989). Electrostatic spraying of liquids in cone-jet mode. *Journal of Electrostatics*, *22*, 135–159.

COMSOL, Inc. (2005) http://www.comsol.com/

Elwenspoek, M., & Jansen, H. V. (1999). *Silicon micromachining*. London: Cambridge University Press.

Fenn, J. B. et al. (1989). Electrospray ionization for mass spectrometry of large biomolecules. *Science*, *246*, 64–71.

Gomez, A. et al. (1997). Production of protein nanoparticles by electrospray drying. *Journal of Aerosol Science*, *29*, 561.

Hendricks, C. D. (1962). Charged droplets experiments. *Journal of Colloid Science*, *17*, 249–259.

Kaelin, M. et al. (2004). Electrosprayed and selenized Cu/In metal particle films. *Thin Solid Films*, *457*, 391–396.

Klemic, K. G. et al. (2002). Micromolded PDMS planar electrode allows patch clamp electrical recordings from cells. *Biosensors of Bioelectronics*, *26*, 597–604.

Kyritsis, D. C., et al. (2002). Mesoscale power generation by a catalytic combustor using electrosprayed liquid hydrocarbons. *Proceedings of the 29th symposium (international) on combustion* (pp. 965–973).

Kyritsis, D. C. et al. (2004). Optimization of a catalytic combustor using electrosprayed liquid hydrocarbons for mesoscale power generation. *Combustion and Flame*, *139*, 77–89.

Lenggoro, I. W. et al. (2000). Preparation of ZnS nanoparticles by electrospray pyrolysis. *Journal of Aerosol Science*, *31*, 121–136.

Liew, L. A. et al. (2001). Ceramic MEMS new materials, innovative processing and future applications. *American Ceramic Society Bulletin*, *80*, 25–30.

Loscertales, I. G., & Fernández de la Mora, J. (1993). In: J. Marijnissen, & S. Pratsinis (Eds.), *Synthesis and characterization of ultrafine particles* Delft: Delft University Press.

Loscertales, I. G. et al. (2002). Micro/Nano encapsulation via electrified coaxial liquid jets. *Science*, *295*, 1695–1698.

Lozano, P. et al. (2004). Electrospray emission from nonwetting flat dielectric surfaces. *Journal of Colloid and Interface Science*, *276*, 392–399.

Mädler, L. et al. (2002a). Controlled synthesis of nanostructured particles by flame spray pyrolysis. *Aerosol Science*, *3*, 369–389.

Mädler, L. et al. (2002b). Rapid synthesis of stable ZnO quantum dots. *Journal of Applied Physics*, *92*, 6538–6540.

Madou, M. (1997). *Fundamentals of microfabrication*. Boca Raton, Florida: CRC Press.

Rulison, A., & Flagan, R. C. (1993). Scale up of electrospray atomization using linear arrays of Taylor cones. *Review of Scientific Instruments*, *64*, 683–686.

Smith, R. D., Barinaga, C. J., & Udseth, H. R. (1988). Improved electrospray ionization interface for capillary zone Electrophoresis-Mass Spectrometry. *Analytical Chemistry*, *60*, 1948–1952.

Tang, K., & Gomez, A. (1994). On the structure of an electrostatic spray of monodisperse droplets. *Physics of Fluids A*, *6*, 2317.

Tang, K., & Gomez, A. (1995). Generation of monodisperse water droplets from electrosprays in a corona-assisted cone-jet mode. *Journal of Colloid and Interface Science*, *175*, 326.

Tang, K., & Gomez, A. (1996). Parametric dependence of electrosprays of low electric conductivity liquids in the cone-jet mode for the generation of monodisperse droplets. *Journal of Colloid and Interface Science*, *184*, 500.

Tang, K. et al. (2001). Generation of multiple electrosprays using microfabricated emitter arrays for improved mass spectrometric sensitivity. *Analytical Chemistry*, *73*, 1658–1663.

Xia, Y. N., & Whitesides, G. M. (1998). Soft lithography. *Annual Review of Materials Science*, *28*, 153–184.

Zeleny, J. (1915). On the conditions of instability of electrified drops, with applications to the electric discharge from liquid points, *Proceedings of the Cambridge Philosophical Society* 18, 71–83.

Zhang, S. et al. (2003). Automated chip-based nanoelectrospray-mass spectrometry for rapid identification of proteins separated by two-dimensional gel electrophoresis. *Electrophoresis*, *24*, 3620–3632.

Zhang, G. et al. (2005). Electrospun nanofibers for potential space-based applications. *Material Science and Engineering B Solid State Materials for Advanced Technology*, *116*, 353–358.